⌘ *Author's Choice*

THE JOURNAL OF BIOLOGICAL CHEMISTRY VOL. 284, NO. 19, pp. 13004–13012, May 8, 2009

Structural and Functional Dissection of the Heterocyclic Peptide Cytotoxin Streptolysin S*[S]

Received for publication, February 4, 2009, and in revised form, March 10, 2009 Published, JBC Papers in Press, March 13, 2009, DOI 10.1074/jbc.M900802200

Douglas A. Mitchell[‡§¶1], Shaun W. Lee[‡§¶], Morgan A. Pence[‖2], Andrew L. Markley[¶], Joyce D. Limm[¶], Victor Nizet[‡‡], and Jack E. Dixon[‡§¶§§3]**

From the Departments of [‡]Pharmacology, [§]Cellular and Molecular Medicine, and [¶]Chemistry and Biochemistry, the [‖]Biomedical Sciences Graduate Program, the [**]Skaggs School of Pharmacy and Pharmaceutical Sciences, Pediatrics, and the [‡‡]Division of Pharmacology and Drug Discovery, University of California, San Diego, La Jolla, California 92093 and the [§§]Howard Hughes Medical Institute, Chevy Chase, Maryland 20815

The human pathogen *Streptococcus pyogenes* secretes a highly cytolytic toxin known as streptolysin S (SLS). SLS is a key virulence determinant and responsible for the β-hemolytic phenotype of these bacteria. Despite over a century of research, the chemical structure of SLS remains unknown. Recent experiments have revealed that SLS is generated from an inactive precursor peptide that undergoes extensive post-translational modification to an active form. In this work, we address outstanding questions regarding the SLS biosynthetic process, elucidating the features of substrate recognition and sites of post-translational modification to the SLS precursor peptide. Further, we exploit these findings to guide the design of artificial cytolytic toxins that are recognized by the SLS biosynthetic enzymes and others that are intrinsically cytolytic. This new structural information has ramifications for future antimicrobial therapies.

Streptolysin S (SLS)[4] is secreted by the human pathogen *Streptococcus pyogenes*, the causative agent of diseases ranging from pharyngitis to necrotizing fasciitis (1). SLS is a potent cytolysin that is ribosomally synthesized, extensively post-translationally modified, and exported to exert its effects on the target cell (2, 3). The expression of SLS promotes virulence in animal models of invasive infection and accounts for the hallmark zone of β-hemolysis surrounding colonies of these bacteria grown on blood agar (2, 4). An intriguing feature of SLS is its nonimmunogenic nature (5). This characteristic is likely due to its small size and its capacity to lyse cells involved in both innate and adaptive immunity (6, 7). The β-hemolytic phenotype of *S. pyogenes* has been studied since the early 1900s, but the molecular structure of SLS has remained elusive (8). In the last decade, transposon mutagenesis studies identified the gene encoding the SLS toxin precursor (*sagA*, for SLS-associated gene) and eight additional genes in an operon required for toxin maturation and export (9). Targeted mutagenesis of the *sag* operon yields nonhemolytic *S. pyogenes* mutants with markedly diminished virulence in mice (2). More recently, it was demonstrated that the protein products of *sagA–D* are sufficient for the *in vitro* reconstitution of cytolytic activity (3). The first gene product, SagA, serves as a structural template that after a series of tailoring reactions matures into the active SLS metabolite (see Fig. 1*A*). A trimeric complex of SagBCD catalyzes these tailoring reactions, which results in the conversion of cysteine, serine, and threonine residues to thiazole, oxazole, and methyloxazole heterocycles, respectively (3).

A DNA gyrase inhibitor, microcin B17, is produced by an orthologous biosynthetic cluster (*mcb*) found in a subset of *Escherichia coli* strains (10–12). Microcin B17 contains four thiazole and four oxazole heterocycles, which are indispensable for biological activity. By analogy to microcin B17 and the lantibiotics, the heterocycles of SLS are formed on the C terminus of SagA, whereas the N terminus serves as a leader peptide (13–15). The installation of thiazole and (methyl)-oxazole heterocycles restricts backbone conformational flexibility and provides microcin B17 and SLS with rigidified structures. The SLS heterocycles are formed via two distinct steps; SagC, a cyclodehydratase, generates thiazoline and (methyl)-oxazoline heterocycles, whereas SagB, a dehydrogenase, removes two electrons to afford the aromatic thiazole and (methyl)-oxazole (3, 16, 17). SagD is proposed to play a role in trimer formation and regulation (see Fig. 1*A*). The final genes in the genetic cluster encode a predicted leader peptidase/immunity protein (SagE), a membrane-associated protein of unknown function (SagF), and three ABC transporters (SagGHI).

It is now appreciated that many other prokaryotes harbor similar genetic clusters for the synthesis of thiazole and (methyl)-oxazole heterocycles (3, 18, 19). Additional important mammalian pathogens such as *Listeria monocytogenes*, *Staphylococcus aureus*, and *Clostridium botulinum*, contain *sag*-like gene clusters that produce SLS-like cytolysins. These toxins are expected to promote pathogen survival and host cell injury during infection, but this has only been conclusively shown for *S. pyogenes* and *L. monocytogenes* (2, 18). Like *E. coli*, many other prokaryotes harbor a *sag*-like genetic cluster but are not known to produce cytolysins. Some examples are the goadsporin-pro-

* This work was supported, in whole or in part, by a National Institutes of Health grant. This work was also supported by grants from the Walther Cancer Institute, the Ellison Foundation, and the Howard Hughes Medical Institute (to J. E. D.).

⌘ *Author's Choice*—Final version full access.

[S] The on-line version of this article (available at http://www.jbc.org) contains supplemental Figs. S1–S3.

[1] Supported by a Hartwell Foundation postdoctoral fellowship.

[2] Supported by the University of California at San Diego Genetics Training Program.

[3] To whom correspondence should be addressed: Howard Hughes Medical Institute, 4000 Jones Bridge Rd., Chevy Chase, MD 20815-6789. Tel.: 301-215-8803; Fax: 301-215-8828; E-mail: jedixon@ucsd.edu.

[4] The abbreviations used are: SLS, streptolysin S; WT, wild type.

ducing organism, *Streptomyces* sp. TP-A0584 and cyanobactin producers such as *Prochloron didemni* (20–22). The molecular targets of these secondary metabolites remain to be elucidated, but it is known that goadsporin exhibits antibiotic activity, and the cyanobactin, patellamide D, reverses multiple drug resistance in a human leukemia cell line (23). Because genetic loci containing *sagBCD*-like genes have been widely disseminated in prokaryotes (3), nature appears to have found a preferred route to synthesizing such secondary metabolites.

In this work, we build upon our initial report on the *in vitro* reconstitution of SLS biosynthesis to uncover the requisite features of substrate selectivity and cytolytic activity. The impetus for defining substrate tolerance arose from earlier results showing that SagBCD accepts alternate substrates *in vitro* (3), as evidenced by two key experiments. First, SagBCD converted a noncognate substrate, ClosA (*C. botulinum*), into a cytolytic entity. Second, mass spectrometry revealed heterocycle formation on the McbA (*E. coli*) peptide after SagBCD treatment (3). Here, we dissect the N-terminal leader peptide and C-terminal protoxin of SagA to define the residues necessary for conversion into SLS.

EXPERIMENTAL PROCEDURES

In Vitro Synthetase Reactions—Protein preparation and synthetase reactions employing maltose-binding protein-tagged substrate and SagBCD were performed as described earlier (3). Membrane damage was quantified by the erythrocyte lysis assay. In every case, omission of the substrate or the SagBCD synthetase resulted in no detectable hemolytic activity (data not shown).

Cytolytic Activity Assay—The *in vitro* and genetic reconstitution assays described below were performed at least three times for each substrate tested. Because of lot-to-lot variation in commercial blood sources and prep-to-prep variation in the specific activity of the synthetase complex, we have elected to report activity semi-quantitatively. *In vitro* hemolytic activity equal to wild type SagA treated with SagBCD is reported as three plus signs (+++). Cytolytic activity that is ~30–70% of wild type SagA is given as (++). Detectable activity that is less than 30% of SagA is thus a single plus sign (+), and nondetectable activity is a single minus sign (−). The cytolytic activity of mutant substrates tested via genetic reconstitution was scored in an analogous manner. All of the assays were internally normalized, and the base line was adjusted using two positive controls (Triton X-100 and wild type SagA treated with SagBCD) and two negative controls (substrate and SagBCD alone).

Transformation and Verification of S. pyogenes M1 sagA Mutants—The *sagA* allelic exchange mutant of *S. pyogenes* M1 was made electrocompetent using a previously published glycine/sucrose method (2). Maxiprepped pDCerm constructs (3 and 12 μg) were incubated with electrocompetent *S. pyogenes* M1 Δ*sagA* and electroporated using an Eppendorf 2510 electroporator set to 1.5 kV. These cells (50 and 150 μl) were then plated on Todd-Hewitt agar plates supplemented with 2 μg/ml erythromycin. Typically, 5–15 colonies would appear ~40 h post-transformation. The insert size was evaluated by screening transformants by colony PCR. Clones harboring an appropriately sized insert were initially screened for cytolytic activity by streaking bacteria on blood agar plates (Hardy Diagnostics). All of the clones were verified to be *S. pyogenes* (Group A *Streptococcus*) by using the BBL Streptocard Enzyme Latex Test (BD Diagnostics).

Cytolytic Assay of Genetically Reconstituted Mutants—Because of the possibility that nonphysiological concentrations could lead to artifactual activity *in vitro*, the cytolytic activity of the peptide substrates were also tested using genetic reconstitution. This method requires that endogenous SagBCD accept the substrate. The method described below does not involve lysing the bacteria. Therefore, mutant substrates must also be proteolytically processed and accepted by the SagGHI export apparatus (ABC transporters). Because of toxicity in *E. coli* and transformation difficulties, intrinsically lytic SagA mutants were not tested by genetic reconstitution. Extracts containing bovine serum albumin-stabilized SLS were prepared in the following manner. Overnight cultures (10 ml) of *S. pyogenes* M1 Δ*sagA* containing pDCerm-*sagA* plasmids were grown to A_{600} ~0.6 in Todd Hewitt broth containing 2 μg/ml erythromycin. The cultures were treated with bovine serum albumin (10 mg/ml) for 1 h at 37 °C and then centrifuged (6,000 × *g*, 10 min) before passing the supernatant through a 0.2-μm acrodisc syringe filter (Pall Corporation). These samples were centrifuged again (6,000 × *g*, 10 min), and the supernatants were assayed for hemolytic activity by addition to defribinated sheep blood (in V-bottom microtiter plates at 1:25 and 1:50 dilutions). The blood was treated for 2–4 h before assessing hemolytic activity as previously reported (3).

Assessment of SLS Mutants in a Murine Skin Infection Model—The experiments were performed using models reported previously (4, 9, 24). *S. pyogenes* M1 Δ*sagA* complemented with *sagA*-WT, *sagA*-S39A, and *sagA*-7C/S were grown to log phase, harvested by centrifugation, washed, resuspended in phosphate-buffered saline, and mixed 1:1 with Cytodex beads (1 mg/ml; Sigma). An inoculum of (1×10^7 colony-forming units in 100 μl) of *S. pyogenes* Δ*sagA* complemented with either *sagA*-S39A or the *sagA*-7C/S mutant was then injected subcutaneously into the right flank of 4-week-old male hairless crl:SKH1(hrhr)Br mice (n = 8/group). *S. pyogenes* Δ*sagA* complemented with *sagA-wt* was injected into the left flank of the same animal for identical comparison. The animals were monitored daily for development of necrotic ulcers. At 4 days post-infection, all of the animals were sacrificed. Biopsies were performed on injection sites for histopathologic assessment (hematoxylin/eosin staining) after measuring the size of tissue ulcers.

Generation of [^{35}S]Met-SagBCD—Radioactive synthetase was prepared using maxiprepped pET28-maltose-binding protein-SagBCD and *in vitro* transcription/translation under T7 promoter control. Rabbit reticulocyte extract (Promega) gave superior yield and purity to wheat germ and S30 extracts. A typical 50-μl reaction was set up as follows: 1–3 μg of plasmid DNA was added to a master mix containing 2 μl of transcription/translation buffer, 25 μl of rabbit reticulocyte extract, 1 μl of RNAsin, 1 μl of minus Met amino acid mix, 1 μl of T7 RNA polymerase, 10 μCi of [^{35}S]Met (PerkinElmer Life Sciences), and DNase/RNase-free water. A small aliquot (0.5 μl) of the radiolabeled product was separated by SDS-PAGE, dried, and

visualized by autoradiography using a Kodak BioMax low energy isotope intensifying screen (20 h, −80 °C).

Peptide Array—Immobilized peptides were synthesized on cellulose membranes using a MultiPep Autospot synthesis robot following the manufacturer's instructions (Intavis AG). Irradiation with 254 nm (UV) light gave an indication of the relative amount of peptide per spot. [^{35}S]Met-SagB, -C, and -D were allowed to bind to the array for 15 h at 4 °C in Tris-buffered saline/Tween 20 (0.1% v/v) supplemented with 2.5% nonfat milk and 2.5% bovine serum albumin (both w/w). The array was then extensively washed with Tris-buffered saline/Tween (4 × 10 min, 23 °C) before exposing film with a Kodak BioMax low energy isotope intensifying screen (20 h, −80 °C). Under these conditions, SagB and SagD did not bind tightly to the array, as indicated by a weak radioactive signal, even after longer exposure times (4 days). Using SagBCD together led to a substantial amount of "radioactive precipitation" on areas of the cellulose membrane that did not contain peptide. Therefore, later experiments were carried out using SagC alone.

RESULTS

The SagA Leader Peptide Provides Substrate Recognition—The precursor peptide from *C. botulinum*, ClosA, shares significant amino acid sequence similarity with SagA (62%) and was converted to a cytolysin by recombinant SagBCD (3). The microcin B17 precursor, McbA, is only moderately similar (32%) but was also accepted as a substrate by SagBCD. Therefore, we hypothesized that SagBCD would accept numerous noncognate substrates (Fig. 1*B*). To demonstrate that the permissive behavior of SagBCD on ClosA was not limited to *in vitro* biochemical studies with purified proteins, genetic complementation studies were performed using a *sagA* deletion mutant produced in an M1 serotype strain of *S. pyogenes* (Δ*sagA*). By transforming this strain with a plasmid encoding the desired peptide substrate, the *in vivo* selectivity of endogenous SagBCD was probed. β-Hemolysis on blood agar was restored when either the wild type *sagA* or *closA* gene was provided to the *S. pyogenes* Δ*sagA* mutant bacteria. To increase sensitivity, we adopted a liquid phase hemolysis assay. Here, the SLS is extracted from the *S. pyogenes* lipoteichoic acid layer using bovine serum albumin as a carrier/stabilizer. This sample is mixed with sheep blood, and the amount of hemoglobin released from lysed erythrocytes is quantified by absorbance. Using this assay, we confirmed that ClosA was converted to a cytolysin by endogenous SagBCD but calculated the level of activity to be reduced by ~⅓ relative to that of SagA (Fig. 1*B*).

Interestingly, the related peptide substrates from *S. aureus* (StaphA) and *L. monocytogenes* (ListA) did not exhibit detectable hemolytic activity with purified recombinant proteins or in genetically complemented *S. pyogenes* Δ*sagA* (Fig. 1*B*). Cotter *et al.* (18) have recently shown that the *sag*-like genetic cluster from *L. monocytogenes* synthesizes an SLS-like cytolytic factor. Therefore, the lack of activity in our assays must originate at the level of substrate recognition or enzymatic tolerance. Previous work from the Walsh laboratory has shown that the N-terminal leader peptide of McbA is required for substrate recognition (14). The most important residues implicated in this process are McbA-F8 and -L12, which are proposed to lie on the same face of an α-helix (15). Alignment with other substrates shows that a similar motif (F*XXX*B, where *X* is any amino acid and B is a branched chain amino acid) is found in the leader peptides of SagA and ClosA but is lacking in StaphA and ListA (Fig. 1*B*). This finding prompted the construction of a double alanine mutant of the F*XXX*B motif (SagA-FIA) and chimeric substrates comprised of the SagA leader peptide fused to the StaphA and ListA C terminus (Fig. 1*C*). If the SagA leader peptide contains adequate substrate recognition information, then activity should be restored upon treating the chimera with purified SagBCD. Furthermore, if the F*XXX*B motif is required for substrate recognition, then cytolytic activity should be reduced for similarly treated SagA-FIA. A full restoration of *in vitro* cytolytic activity was observed for both the SagA-ListA and SagA-StaphA chimera. In contrast, genetic complementation revealed that only SagA-StaphA retained activity, indicating that either the endogenous rules of cytolytic conversion are more restrictive or the SagA-ListA substrate is not efficiently exported. Enzymatic promiscuity could theoretically be amplified *in vitro* by the presence of large amounts of purified SagBCD. This is supported by the observation that SagA-FIA has detectable activity using purified enzymes but not under genetic reconstitution conditions (Fig. 1*C*).

Unnatural SagA analogs were prepared to shed light on the positional requirements of heterocycle formation. We first designed an artificial substrate, SagX, in an attempt to assess the minimum features for the formation of a cytolysin. Four criteria were used to design this potential substrate: (i) the SagA leader peptide to provide recognition, (ii) a stretch of contiguous heterocyclizable residues adjacent to the leader peptide cleavage site, (iii) 30% glycine evenly distributed through the C-terminal half, and (iv) a serine flanked by two glycine residues. Akin to SagA-ListA, this artificial substrate gave activity equal to SagA in the *in vitro* assay but no activity upon complementation of the Δ*sagA* mutant of *S. pyogenes*. The region of SagA between the cysteine-rich region and the last heterocyclizable residue (^{33}FSIA…GSYT^{50}) was further probed by designing two additional unnatural substrates. SagA inverse simply inverted residues 33–50 of SagA, whereas in SagA scramble this region was reordered in a randomized fashion. Despite having the highest protoxin similarity to wild type SagA, the SagA inverse substrate did not yield lytic activity in either assay. SagA scramble was active *in vitro* but did not complement hemolytic activity in *S. pyogenes* Δ*sagA*. These data show that the leader peptide, especially the F*XXX*B motif, is important for substrate acceptance and that heterocyclizable positions must be available at precise positions to allow creation of an SLS-like cytolytic factor. Additionally, these data indicate that even though SagBCD accepts artificial substrates, there is a limit to the enzymatic promiscuity. These limits are more pronounced during genetic complementation experiments most likely because substrate recognition and enzymatic tolerance are bypassed to an extent when using purified SagBCD. An alternative explanation is that the unnatural substrates are secreted from *S. pyogenes* with differing efficiencies.

Analysis of SagA Leader Peptide Binding Requirements—Because the above activity assays measure both substrate binding and heterocycle formation in a simultaneous and indirect fash-

A

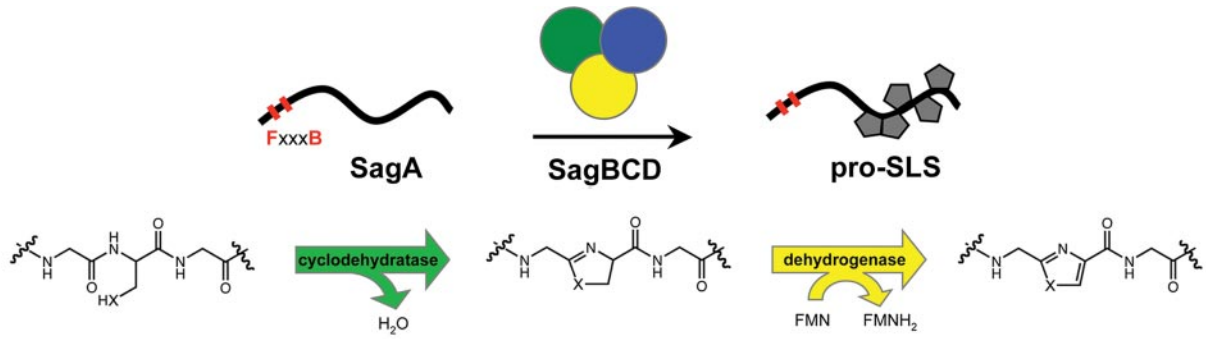

B

Substrate	Wild-type Sequence	Full-length Similarity (%)	Lytic Activity *In vitro*	Lytic Activity *In vivo*
SagA	MLKFTSNILATSVAETTQVAPGG*CCCCCTTCCFSIATGSGNSQGGSGSYTPGK	100	+++	+++
ClosA	MLKFNEHVLTTTNNSNNKVTVAPG*SCCCCSCCCCVSVSVGGGSASTGGGAAAGQGGN	62	+++	++
StaphA	MMKINNHTINGYSDINSSEAMQYAAG*CCSCSCSCSCSCSCSCTSASTAEQ	46	-	-
ListA	MNIKSQSSNGYSNNAVGSEAMNYAAG*CCSCSCSTCTCTCTCASSAATKM	44	-	-
McbA	MELKASEFGVVLSVDALKLSRQSPLG–VGIG$_{10}$SCGGQGGGCGGCSNGCSGGNGGSGGSGSHI	32	n.a.	n.a.

FxxxB Leader peptide — Protoxin

C

Substrate	Mutant Sequence	Protoxin Similarity (%)	Lytic Activity *In vitro*	Lytic Activity *In vivo*
SagA-FIA	MLKATSNALATSVAETTQVAPGG*CCCCCTTCCFSIATGSGNSQGGSGSYTPGK	100	+	-
SagA-StaphA	MLKFTSNILATSVAETTQVAPGG*CCSCSCSCSCSCSCSCTSASTAEQ	50	+++	+++
SagA-ListA	MLKFTSNILATSVAETTQVAPGG*CCSCSCSTCTCTCTCASSAATKM	45	+++	-
SagX	MLKFTSNILATSVAETTQVAPGG*CCCCGGIAGAINGGSGGSYTPNK	57	+++	-
SagA-inverse	MLKFTSNILATSVAETTQVAPGG*CCCCCTTCCTYSGSGGQSNGSGTAISFPGK	68	-	-
SagA-scramble	MLKFTSNILATSVAETTQVAPGG*CCCCCTTCCNSGGFGSATYSSQGGSTIPGK	60	++	-

FIGURE 1. **SagBCD substrate recognition is provided by the SagA leader peptide.** *A*, SagA is converted into an active cytolysin, pro-streptolysin-S (*pro-SLS*), by the actions of SagBCD (a trimeric oxazole/thiazole synthetase). Heterocycles are schematically represented as *shaded pentagons*. A marginally conserved motif in the SagA leader peptide, F*XXX*B (where B is a branched chain amino acid), is highlighted in *red*. Individual reactions catalyzed by SagC (cyclodehydratase) and SagB (FMN-dehydrogenase) are shown. *B*, representative amino acid sequences and cytolytic activity of SagA-like substrates. Shown in *red* are leader peptide residues that comprise the F*XXX*B motif. The putative leader peptide cleavage sites are shown as *asterisks*, except for McbA, where the site is known (*hyphen*). In *blue* are sites of potential heterocycle formation (for McbA, known sites are *blue*). The percentage of amino acid similarity to full-length SagA (as determined by ClustalW alignment) is given. The cytolytic activity was tested for these substrates *in vitro* using purified proteins and *in vivo* using the SLS-deficient strain, *S. pyogenes* Δ*sagA*, complemented with the desired substrate. Activity equal to wild type SagA is designated as (+++); activity that is 30–70% of wild type SagA is (++); detectable activity that is less than 30% of SagA is noted as (+); and nondetectable activity is (−). The activity for McbA is not applicable (*n.a.*) because this secondary metabolite is a DNA gyrase inhibitor, not a cytolysin. *C*, sequences and lytic activity of mutant substrates. All of the substrates contain the wild type SagA leader peptide, except for the first entry (F*XXX*B mutant, SagA-FIA). The percentage of amino acid similarity to the protoxin half of SagA is shown. The second and third entries are SagA leader peptides fused to the protoxin of StaphA and ListA. SagX is an artificially designed toxin, whereas the inverse and scrambled substrates manipulate the sequence of SagA between residues 33–50 (*underlined*).

ion, peptide arrays were synthesized to directly evaluate binding. Based on a perceived importance of the F*XXX*B motif in SagBCD substrate acceptance, the first array consisted of a panel of leader peptides that contain the F*XXX*B motif. Next to each wild type (WT) sequence, the F*XXX*B double alanine mutation was synthesized for SagA, ClosA, McbA, and a substrate from *Pyrococcus furiosus*, designated PagA (Fig. 2*A*). Equal peptide loading was confirmed by irradiating the array with UV (254 nm) light. To assess binding, [^{35}S]Met-labeled SagBCD was prepared by *in vitro* transcription/translation (supplemental Fig. S1) and allowed to interact with the peptide array as described under "Experimental Procedures." Initially, the SagBCD complex was tested for binding in approximately a 1:1:1 ratio, as judged by the number of methionines and the intensity of exposure. Unfortunately, this led to a substantial amount of precipitation that could not be removed from the cellulose membrane and rendered the binding information unreliable. Therefore, SagB, SagC, and SagD were tested individually for binding. SagB and SagD did not bind tightly to the leader peptide array and were washed off before exposing the film (data not shown). SagC, however, bound with high affinity to the array. For the WT sequences, SagC binding was highest to SagA, followed by ClosA and PagA (Fig. 2*A*). Binding to McbA was the weakest, as measured by autoradiographic intensity. Importantly, binding to each F*XXX*B mutant was reduced in comparison with the corresponding WT leader peptide.

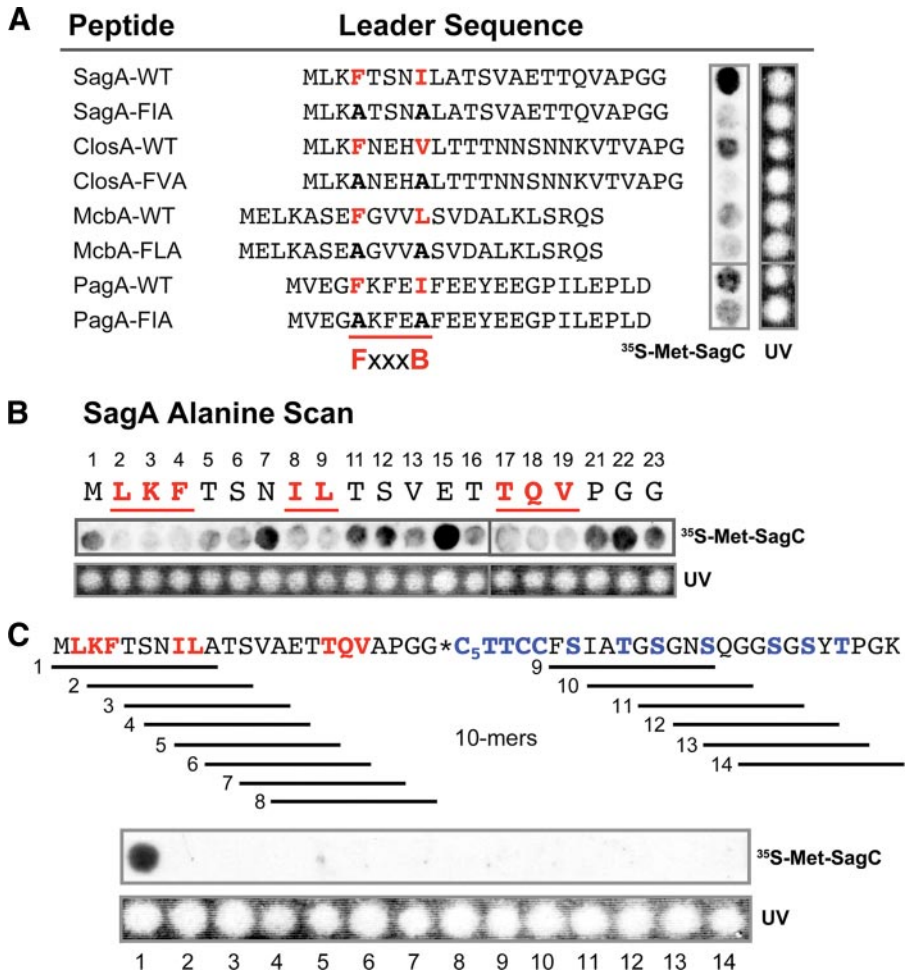

FIGURE 2. **Elucidation of the SagC binding determinants.** *A*, using a peptide array synthesizer, the given sequences were generated with C-terminal attachment to a cellulose membrane. The F*XXX*B motif was left intact (WT) and mutated to Ala for the substrates from *S. pyogenes* (SagA), *C. botulinum* (ClosA), *E. coli* (McbA), and *P. furiosus* (PagA). [^{35}S]Met-SagC was allowed to bind to the array before extensive washing and exposure to film. The relative binding of SagC to the array is indicated by the autoradiographic exposure. Equal peptide loading is confirmed by UV irradiation (254 nm). *B*, the SagA leader peptide alanine scan array was synthesized to obtain positional contributions to SagC binding. The putative leader peptide of SagA contains three alanines (3 of 23); therefore 20 mutants of SagA were tested in this assay. The residue number, amino acid mutated to alanine, relative binding of [^{35}S]Met-SagC (autoradiography), and peptide loading control (UV) are aligned. Positions found to be important for binding are shown in *red*. Positions 2–4, 8, and 9 contain the F*XXX*B motif; positions 17–19 comprise the TQV motif. *C*, a peptide array comprised of fourteen 10-mer peptides of SagA was prepared to evaluate the binding contributions of each interaction site within the leader and the protoxin C terminus. The entire length of SagA is represented, except for the middle cysteine-rich region. Relative binding and peptide loading are demonstrated as above.

The FXXXB Leader Motif Is Necessary but Not Sufficient for SagC Recognition—Although the F*XXX*B motif is an important determinant for directing SagC substrate binding, it does not contribute all of the interaction energy. This is illustrated by the observation that SagC bound to the SagA-WT leader peptide more efficiently than the other WT peptides (Fig. 2*A*). Furthermore, simple incorporation of F*XXX*B into the StaphA and ListA leader peptide did not provide sufficient affinity to detect SagC binding by this method (data not shown). These observations led to the hypothesis that additional residues of SagA contribute to SagC binding.

To elucidate these binding determinants, a second array was synthesized that consisted of an alanine scan of the SagA leader peptide (Fig. 2*B*). Each residue of SagA that is not naturally found as alanine was individually mutated to alanine and tested for SagC binding as above. As expected, mutation to alanine did not disrupt SagC affinity at every location. However, the binding levels were significantly reduced when residues comprising the F*XXX*B motif were mutated (Phe^4 and Ile^8). It was also found that residues adjacent to the F*XXX*B sequence (Leu^2, Lys^3, and Leu^9) and another binding site (Thr^{17}, Gln^{18}, and Val^{19}) were also critical for SagC binding (Fig. 2*B*).

An additional array was used to ascertain the contribution of each interaction site found in the leader peptide and to also assess whether the C-terminal region of SagA plays a role in binding. A panel of fourteen 10-mer peptides were included in the array that scan the full-length of SagA, except for the oxidatively prone, and synthetically challenging, cysteine-rich region (Fig. 2*C*). After binding SagC to this array, it was found that only the first peptide was capable of providing enough binding information to retain SagC through the washing steps. Peptide 1 comprises residues 1–10 of SagA and not only contains the F*XXX*B motif but also the important adjacent residues (Leu^2, Lys^3, Phe^4, Ile^8, and Leu^9). Peptide 5 contains Ile^8 and Leu^9 but only the first residue of the TQV site (The^{17}). This peptide is insufficient at retaining SagC. Taken together, these findings demonstrate that separate sites within the N-terminal leader peptide synergize to provide SagC with a high affinity binding site.

Binding parameters for the SagA-WT, SagA-FIA (F*XXX*B double alanine mutant), and SagA-TQV (triple alanine mutant) leader peptides with SagC were then measured by surface plasmon resonance to quantify the contribution of each binding motif. Using a C-terminal hexahistidine tagged version of SagA-WT, -FIA, and -TQV, the rates of association (k_a) and dissociation (k_d) were first measured with SagC (Table 1). A typical sensorgram and curve fitting analysis are provided in supplemental Fig. S2. As expected from the peptide array data, the effects of F*XXX*B and TQV mutation were substantial. Compared with SagA-WT, SagC bound to the SagA-FIA peptide ~16-fold less tightly. The reduction in affinity was accounted for by an increased k_d (k_a was unchanged). SagC affinity for SagA-TQV was also reduced (~24-fold). The major factor in the SagA-TQV mutant reduction in affinity is an increased k_d; however, there is also a slight

decrease in k_a (<2-fold) upon comparison with SagA-WT (Table 1).

We next determined whether the rules of substrate recognition applied to other cyclodehydratases. ClosC and McbB, from *C. botulinum* and *E. coli*, respectively, were tested for SagA binding. Relative to SagC, binding to the SagA-WT leader peptide was reduced with both ClosC and McbB (~12- and ~130-fold, respectively; Table 1). This trend correlates with the degree of amino acid similarity to SagC (59% for ClosC; 28% for McbB). Mutation of the SagA F*XXX*B and TQV motifs led to additional losses of affinity in the same manner as for SagC binding (*i.e.* both the F*XXX*B and TQV mutants effect k_d; the k_a is only slightly affected by the mutation of TQV). This suggests that although each cyclodehydratase is likely fine-tuned for a single endogenous substrate, the substrate binding mechanism is conserved across species.

TABLE 1

Contribution of SagA interaction sites to cyclodehydratase binding kinetics

Surface plasmon resonance was performed using leader peptides of SagA with a C-terminal His_6 tag as the immobilized ligand. The sequences of the peptides are as follows: SagA-WT, MLKFTSNILATSVAETTQVAPGGHHHHHH; SagA-FIA, MLK**A**TSN**A**LATSVAETTQVAPGGHHHHHH; SagA-TQV, MLKFTSNILATSVAET**AAA**APGGHHHHHH. The underlined residues indicate SagC-binding motifs. The analytes tested for binding were the cyclodehydratases from *S. pyogenes* (SagC), *C. botulinum* (ClosC), and *E. coli* (McbB). The association rates (k_a) and dissociation rates (k_d) were recorded in duplicate at two concentrations and used to calculate the dissociation constant (K_D). The error is reported as standard deviation of the mean. The χ^2 values are given as an assessment of curve fitting accuracy.

Ligand	Analyte	k_a ($\times 10^3$)	k_d ($\times 10^{-4}$)	K_D	χ^2
		$M^{-1}s^{-1}$	s^{-1}	nM	
SagA-WT	SagC	3.7 ± 0.4	0.25 ± 0.03	6.7 ± 0.8	0.04
SagA-FIA	SagC	3.7 ± 0.3	3.5 ± 0.3	95 ± 7.0	0.04
SagA-TQV	SagC	2.1 ± 0.3	3.4 ± 0.8	160 ± 30	0.03
SagA-WT	ClosC	3.8 ± 0.3	3.1 ± 0.7	82 ± 14	0.10
SagA-FIA	ClosC	3.3 ± 0.5	7.2 ± 1.0	220 ± 30	0.07
SagA-TQV	ClosC	2.5 ± 0.3	9.6 ± 0.9	380 ± 40	0.03
SagA-WT	McbB	2.5 ± 0.3	22 ± 4.0	880 ± 140	0.58
SagA-FIA	McbB	2.3 ± 0.2	27 ± 1.0	1200 ± 100	0.25
SagA-TQV	McbB	2.0 ± 0.3	41 ± 5.2	2100 ± 310	0.04

Mutational Analysis of Heterocyclizable Residues of SagA—Numerous attempts at identifying sites of heterocycle formation on SagA by mass spectrometry have failed. As a result, a site-directed mutagenesis approach was initiated to determine functionally important residues of SagA with the assumption that the lack of cytolytic activity by particular SagA point mutants is suggestive of heterocycle locations. To begin this study, every heterocyclizable residue (cysteines, serines, and threonines) located on the protoxin half of SagA (residues 24–53) was individually mutated. Cysteines and serines were mutated to alanines, whereas threonines were mutated to valines, a closer structural mimic. The lytic activity of these proteins was assessed *in vitro* after treatment with purified SagBCD and through genetic complementation of *S. pyogenes* Δ*sagA*. Each mutation was classified as having no effect (mutant SLS was fully active), a contributing effect (reduced activity), or a critical effect (inactive). Using these two independent assays, key functional residues of SLS were identified. It is important to note that our method of testing the cytolytic activity of SagA point mutants through genetic complementation measures activity and secretion in a simultaneous fashion.

Compiled results are overlaid on the amino acid sequence of SagA (Fig. 3*A*) and are also provided in table form (Fig. 3*B*). This

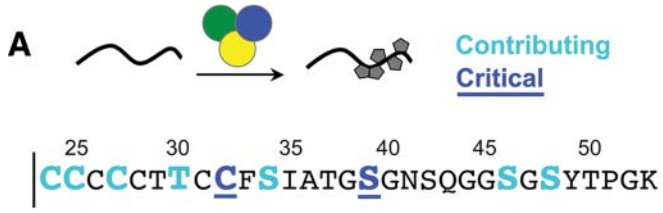

B

SagA Mutant	Lytic Activity *In vitro*	Lytic Activity *In vivo*	SagA Mutant	Lytic Activity *In vitro*	Lytic Activity *In vivo*
WT	+++	+++	T37V	+++	+++
C24A	++	-	S39A	-	-
C25A	++	+	S39C	++	n.d.
C26A	+++	++	S39P	++	++
C27A	++	+	S42A	+++	+++
C28A	+++	+++	S46A	++	+
T29V	+++	+++	S48A	++	++
T30V	++	++	T50V	+++	+++
C31A	+++	+++	2C/S[a]	-	-
C32A	-	-	3C/S[a]	-	-
C32P	++	n.d.	7C/S[a]	-	-
C32S	++	n.d.	4T/V[a]	-	-
S34A	+	+			

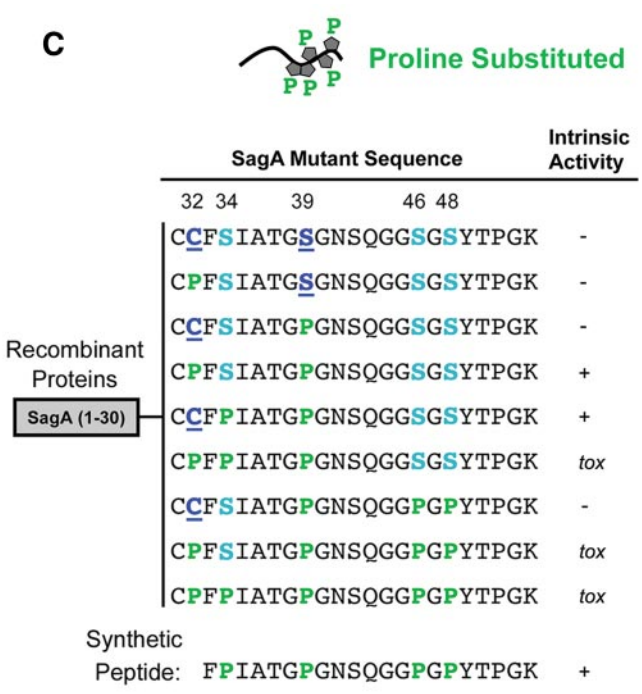

FIGURE 3. **Identification of SagA residues necessary for cytolytic activity.** *A*, compilation of the cytolytic data for SagA point mutations after reaction with SagBCD. Residues that are C-terminal to the predicted leader peptide cleavage site (*vertical line*) of SagA (24–53) are shown. Positions that contribute to cytolytic activity are shown in *light blue*. The positions critical for cytolysis are *dark blue* and *underlined*. *B*, the activity of each SagA mutant was tested by the erythrocyte lysis assay *in vitro* using purified proteins and *in vivo* by genetic complementation. Activity scoring is as in Fig. 1*B*. [a] Multiple sites were mutated. 2C/S, C31S/C32S; 3C/S, C26S/C27S/C28S; 7C/S, all seven cysteines mutated to serine; 4T/V, all four threonines mutated to valine. *C*, the intrinsic activity of SagA substituted with proline was tested using purified protein. No SagBCD was used in this assay. Toxicity (*tox*) was observed for some SagA proline mutants, which prevented recombinant expression. A synthetic peptide was prepared to test proline substitution at each serine found to be important for SagA activity.

analysis revealed that not all sites of potential heterocycle formation were important for activity, but most mutations had a measurable impact on function. Two mutations, C32A and S39A, completely abolished the cytolytic activity of SLS in both assays and are thus highly likely sites of thiazole/oxazole formation. Moreover, it was found that serine and cysteine could substitute for one another at these two critical sites (C32S and S39C) with a small reduction of *in vitro* activity. However, serine cannot be used to replace multiple adjacent cysteines as indicated by the lack of activity in C31S/C32S (2C/S), C26S/C27S/C28S (3C/S), and a total serine (7C/S) mutant (Fig. 3*B*). Similarly, valine cannot completely replace threonine (4T/V).

Overall, the activities measured by *in vitro* reconstitution and genetic complementation agreed. The one case were the assays did not concur was with the C24A mutation. We observed substantial lytic activity *in vitro* but no activity in genetically complemented bacteria (Fig. 3*B*). This residue is predicted to flank the leader peptide cleavage site. We have previously shown that leader peptide removal is not required for *in vitro* activity (3). Thus, a reduction of activity in genetic complementation experiments may result from reduced leader peptide processing and/or secretion. These results confirm that many residues within SagA are important for activity and predict that SLS is highly post-translationally modified.

Proline Can Substitute for Thiazoles and Oxazoles in the SagA Propeptide—We rationalized that because thiazoles and oxazoles are five-membered, nitrogen-containing heterocycles that restrict peptide backbone conformation, proline may be capable of serving as a structural mimic. Therefore, the SagA-C32P and -S39P mutants were prepared and treated with purified SagBCD. These yielded substantial *in vitro* lytic activity (Fig. 3*B*) and encouraged the construction of SagA mutants that were cytolytic in the absence of SagBCD. Thus, proline was systematically incorporated into select heterocyclizable sites of SagA that were previously determined to be important for activity (positions 32, 34, 39, 46, 48). This proline-substituted SagA panel was then tested for lytic activity in the absence of SagBCD (Fig. 3*C*). Wild type SagA and two single substituted proline mutations (C32P and S39P) did not exhibit intrinsic lytic activity. In contrast, two double proline substituted mutants showed dose-dependent activity without SagBCD treatment (C32P/S39P and S34P/S39P) (Fig. 3*C* and supplemental Fig. S3). A triple mutant, C32P/S34P/S39P, predicted to further enhance lytic activity, killed *E. coli* upon induction of protein expression and yielded no protein. Likewise, additional permutations revealed that if either Cys^{32} or Ser^{34} are substituted in combination with Ser^{39}, Ser^{46}, and Ser^{48}, *E. coli* toxicity was encountered. To support the claim that toxicity arose because of SLS-like activity, a synthetic peptide comprised of the C-terminal 21 residues of SagA was synthesized with prolines at positions 34, 39, 46, and 48. This peptide, although devoid of cysteine, was intrinsically lytic in a dose-dependent manner (Fig. 3*C* and supplemental Fig. S3). The observation that select proline mutations endow SagA with intrinsic lytic activity bolsters the conclusion that the above sites are heterocyclized in SLS.

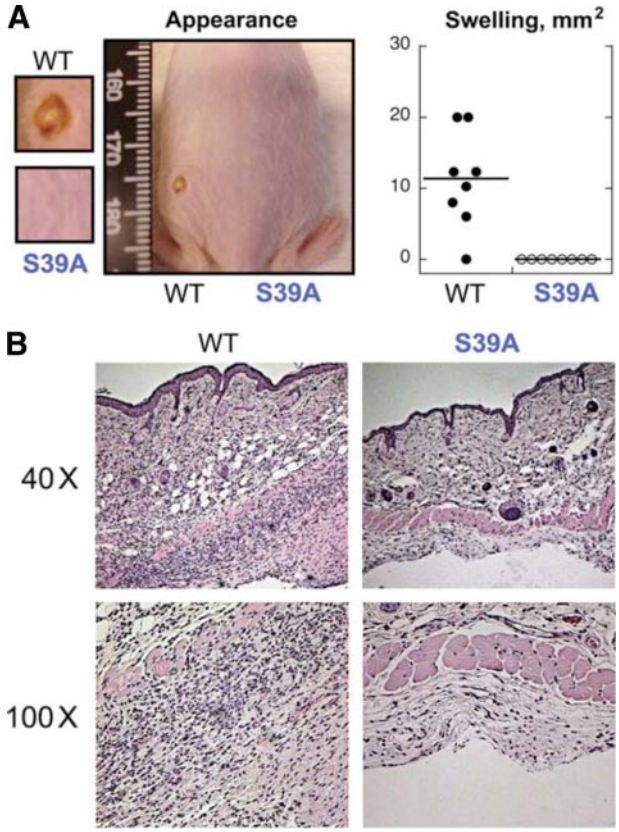

FIGURE 4. **Ser^{39} of SagA is required for virulence in a mouse infection model.** *A*, 4-week-old hairless crl:SKH1(hrhr)Br mice were challenged subcutaneously with 10^7 colony-forming units of *S. pyogenes* M1 Δ*sagA* complemented with *sagA*-WT (*left flank*) and *sagA*-S39A (*right flank*). Gross appearance of a typical mouse and lesion size (mm^2) are shown at 4 days post-inoculation. The *insets* on the *left* show closer views of the injection sites. A necrotic ulcer is visible with *sagA*-WT. No lesions are visible with *sagA*-S39A. *B*, histological evaluation (hemotoxilyn/eosin staining) of excised tissue from site of injection. Magnification is given at 40× and 100×.

Key Heterocycles of SLS Are Required for S. pyogenes Virulence in Mice—To determine the importance of heterocyclic conversion of SLS for disease progression, mice were subcutaneously injected with *S. pyogenes* M1 Δ*sagA* mutant complemented with either *sagA*-WT, *sagA*-S39A, or *sagA*-7C/S. Seven of eight mice infected with the *sagA*-WT complemented strain developed significant necrotic ulcers and swelling, whereas no change was observed in any infections of *sagA*-S39A (Fig. 4*A*) and *sagA*-7C/S (data not shown). Histological examination of tissues from WT and the mutant infections shows that WT infections exhibit more extensive tissue disruption and a higher infiltration of neutrophils (Fig. 4*B*). These results demonstrate that a single SagA point mutation predicted to interfere with heterocycle formation markedly reduces the virulence of *S. pyogenes* in a murine model of skin infection.

DISCUSSION

For SagA to be converted into the active SLS cytolysin, the SagBCD synthetase complex must first recognize the SagA substrate. Heterocycles must then be installed at the proper locations to elicit biological activity. By using two independent assays, we analyzed the substrate permissivity of SagBCD using *in vitro* biochemical assays and genetic reconstitution. The sub-

strate tolerance of SagBCD was initially assessed using substrates from other members of the firmicutes phylum that were suspected of producing SLS-like cytolysins. To begin, we chose the substrate from *C. botulinum*, which harbors the most highly related *sag*-like genetic cluster (*clos*A-I) known outside of the *Streptococcus* genus. SagBCD accepted ClosA as a noncognate substrate *in vitro* and in genetically complemented *S. pyogenes* Δ*sagA* bacteria, but the activity was reduced relative to SagA (Fig. 1*A*). This could stem from a number of possibilities. The most likely explanation, in light of our binding data, is that SagBCD process ClosA more slowly because of a lowered substrate affinity. *In vitro*, ClosA treated with purified SagBCD resulted in activity equal to SagA. However, under the conditions employed, nonphysiological concentrations of synthetase and substrate could easily result in an elevated level of substrate permissivity. Other explanations for reduced ClosA activity upon genetic reconstitution could be that on a molar basis SLS is more potent or that the leader peptidase and/or export machinery process the toxin more slowly. If the latter was true, toxicity would be an expected outcome, but analysis of growth curves indicated that this is not the case (data not shown).

Because ClosA and McbA were both known *in vitro* substrates of the SagBCD synthetase (3), we were initially surprised when SagBCD rejected potential substrates more similar to SagA than McbA (*i.e.* StaphA and ListA; Fig. 1*B*). However, chimeric substrates consisting of the SagA leader peptide coupled with the StaphA or ListA protoxin were fully active *in vitro* after treatment with recombinant SagBCD. This indicated that the SagA leader peptide conferred substrate recognition to SagBCD. Later experiments showed that a partially conserved motif in the SagA leader peptide, F*XXX*B, played a major role in efficient cytolytic conversion (Fig. 1*C*) and SagC affinity (Fig. 2 and Table 1). Additionally, the SagA leader peptide can be fused to properly designed artificial protoxins to yield cytolysins after treatment with SagBCD.

Peptide array binding experiments uncovered that in addition to the F*XXX*B motif and some adjacent residues, SagC also recognizes another site (TQV) on the SagA leader peptide (Fig. 2). Given that the K_D was measured to be in the low nanomolar range, multiple binding sites on SagA would be presumed necessary to drive such an avid interaction (Table 1). Mutation of the SagA-TQV site led primarily to an increased k_d with a modest decrease of k_a relative to SagA-WT (Table 1). This is in contrast to the SagA-FIA mutant, which only led to an increased k_d. These binding trends also held for the SagA binding interaction with the cyclodehydratases from a closely related organism (*C. botulinum*, ClosC) and a distantly related organism (*E. coli*, McbB; Table 1). We hypothesize this relationship will be true of all *sag*-like clusters that harbor substrates with F*XXX*B motifs in the leader peptide.

Elucidation of the SagC substrate recognition requirements was undertaken to judge why certain substrates are accepted by the SagBCD synthetase and why others are not. Earlier studies have demonstrated that the SLS precursor from a fish pathogen, *Streptococcus iniae*, was able to complement the hemolytic activity of *S. pyogenes* Δ*sagA* (25, 26). Upon comparison with SagA from *S. pyogenes*, the *S. iniae* leader peptide has a single mutation in the leader sequence (K3Q). Thus, it should not be surprising that SagA from *S. iniae* was an efficient substrate of *S. pyogenes* SagBCD. We conclude that ClosA was accepted by recombinant and endogenous SagBCD because of a complete F*XXX*B site (LKF and VL) and a partial TQV site (Val^{19}). Previous results has also shown that SagBCD accepts McbA as a substrate (3). This is supported by the present work demonstrating that SagC directly binds to the McbA leader peptide (Fig. 2*A*). Relative to SagA, the SagC binding to McbA was greatly reduced, but the data provide a satisfactory explanation; the leader peptide of McbA contains partial SagC-binding sites. The F*XXX*B sequence is present, but the important surrounding residues are nonconservatively mutated. Also, the Gln of the TQV site is present (Fig. 2*A*).

The identification of the TQV site helps explain why simple inclusion of F*XXX*B into the StaphA and ListA leader peptides did not result in high affinity SagC binding. Residues adjacent to the F*XXX*B motif (LKF and IL) also contribute to this interaction. Of a total 23 residues in the predicted SagA leader peptide, eight are directly involved in driving substrate affinity. This implies that upon SagC binding SagA, nearly the entire length of the leader peptide will be associated, possibly buried, in a SagC-binding site. Undoubtedly, the extended recognition capability of SagC acts to prevent the synthetase complex from processing unwanted peptides/proteins. Perhaps this affinity is also a protective measure employed by *S. pyogenes*. Our work has demonstrated that pro-SLS (Fig. 1*A*) is highly active, and it is possible that a tightly bound synthetase complex will cage the activity until the metabolite is ready for export.

SLS has historically been recalcitrant to isolation and characterization. However, the early work of Bernheimer (27, 28), Bernheimer and Schwartz (29), and Koyama (30–32) shed important light on the nature and action of SLS. Using gel filtration analysis on partially purified SLS, Bernheimer (33) predicted that the molecular weight of the polypeptide would be 2.8 kDa. This is quite remarkable, given that a modern calculation of 2.7 kDa is based on modifications to SagA, a peptide discovered over 30 years later. Our results suggest that in the mature structure of SLS, oxazoles will be formed from SagA residues Ser^{34}, Ser^{39}, Ser^{46}, and Ser^{48} (Fig. 3*B*). The work of Kolter and co-workers (10–12) on microcin B17 provides a literature precedent for heterocycle formation when the preceding residue is glycine (Ser^{39}, Ser^{36}, and Ser^{48}) (34, 35). Presumably, the increased flexibility in the peptide backbone at these locations facilitates the orbital alignment required for cyclodehydration. Oxazole formation at the abovementioned sites is further supported by the creation of proline-substituted SagA mutants that exhibit intrinsic cytolytic activity (Fig. 3*C*).

Our mutagenesis data confirm a previous study identifying SagA Cys^{24} and Cys^{27} as residues important for the activity of SLS on blood agar plates (2). Despite this, the fate of the cysteine-rich region (Cys^{24}–Cys^{32}) remains speculative. Given the observation that C32S and C32P were cytolytic, we expect Cys^{32} to be converted to a thiazole. However, serine cannot simultaneously substitute for multiple adjacent cysteines. This implies that there is either a polythiazole-specific electronic contribution to cytolysis or that another type of modification is present in the mature structure of SLS. Our current data cannot distinguish between these two possibilities, which will require

extensive methodology improvements. We hypothesize that it is unlikely free thiols, disulfides, or lanthionines will be present in the final SLS structure. This is because SLS is known to be oxygen-stable (36, 37), and cysteine was not detected in an amino acid analysis study (30). Moreover, the *sagA-I* cluster, which is sufficient to confer SLS production to a heterologous bacterial species (4), does not harbor the appropriate dehydratases and cyclases to form lanthionine linkages (4, 38, 39).

The murine infection study supports our previous data that SLS heterocycle formation is required for the virulence of *S. pyogenes*. Furthermore, we show that a single amino acid change, SagA-S39A, renders this pathogen avirulent in a skin infection model (Fig. 4). Without active SLS, the bacteria exhibit undetectable pathogenicity and are efficiently cleared by the murine immune system. It is conceivable that in such a setting, antibodies could be raised against inactive SLS mutants. Whether this represents a viable strategy for vaccine development remains to be seen, but with the tactical role SLS-like toxins play in pathogenesis, further study is warranted.

This study has elucidated the requisite features of SagBCD substrate recognition and SagA residues of functional importance. We conclude that although the C terminus of SagA undergoes enzymatic conversion, only the N-terminal leader peptide substantially contributes to substrate recognition. Conceivably, these principles could be used to guide the design of other artificial toxins for antibiotic or anticancer applications. Additionally, our study has yielded a wealth of structure-activity data on a conserved family of bacterial virulence factors and lays the foundation for the development of a structure-based vaccine.

Acknowledgments—We thank C. J. Allison (S. Taylor Lab, University of California at San Diego) for preparing the peptide arrays and Jill Harrington (Kolodner Lab, University of California at San Diego) for assistance with the Biacore T100. We are grateful to members of the Dixon lab and Mary Hensler for helpful discussions.

REFERENCES

1. Nizet, V. (2002) *Trends Microbiol.* **10,** 575–580
2. Datta, V., Myskowski, S. M., Kwinn, L. A., Chiem, D. N., Varki, N., Kansal, R. G., Kotb, M., and Nizet, V. (2005) *Mol. Microbiol.* **56,** 681–695
3. Lee, S. W., Mitchell, D. A., Markley, A. L., Hensler, M. E., Gonzalez, D., Wohlrab, A., Dorrestein, P. C., Nizet, V., and Dixon, J. E. (2008) *Proc. Natl. Acad. Sci. U. S. A.* **105,** 5879–5884
4. Nizet, V., Beall, B., Bast, D. J., Datta, V., Kilburn, L., Low, D. E., and De Azavedo, J. C. (2000) *Infect. Immun.* **68,** 4245–4254
5. Robinson, J. (1951) *J. Immunol.* **66,** 661–665
6. Ofek, I., Bergner-Rabinowitz, S., and Ginsburg, I. (1972) *Infect. Immun.* **6,** 459–464
7. Hryniewicz, W., and Pryjma, J. (1977) *Infect. Immun.* **16,** 730–733
8. Marmorek, A. (1895) *Ann. Inst. Pasteur* **9,** 593–620
9. Betschel, S. D., Borgia, S. M., Barg, N. L., Low, D. E., and De Azavedo, J. C. (1998) *Infect. Immun.* **66,** 1671–1679
10. Yorgey, P., Davagnino, J., and Kolter, R. (1993) *Mol. Microbiol.* **9,** 897–905
11. Yorgey, P., Lee, J., Kordel, J., Vivas, E., Warner, P., Jebaratnam, D., and Kolter, R. (1994) *Proc. Natl. Acad. Sci. U. S. A.* **91,** 4519–4523
12. Li, Y. M., Milne, J. C., Madison, L. L., Kolter, R., and Walsh, C. T. (1996) *Science* **274,** 1188–1193
13. de Vos, W. M., Kuipers, O. P., van der Meer, J. R., and Siezen, R. J. (1995) *Mol. Microbiol.* **17,** 427–437
14. Madison, L. L., Vivas, E. I., Li, Y. M., Walsh, C. T., and Kolter, R. (1997) *Mol. Microbiol.* **23,** 161–168
15. Roy, R. S., Kim, S., Baleja, J. D., and Walsh, C. T. (1998) *Chem. Biol.* **5,** 217–228
16. Milne, J. C., Roy, R. S., Eliot, A. C., Kelleher, N. L., Wokhlu, A., Nickels, B., and Walsh, C. T. (1999) *Biochemistry* **38,** 4768–4781
17. Roy, R. S., Gehring, A. M., Milne, J. C., Belshaw, P. J., and Walsh, C. T. (1999) *Nat. Prod. Rep.* **16,** 249–263
18. Cotter, P. D., Draper, L. A., Lawton, E. M., Daly, K. M., Groeger, D. S., Casey, P. G., Ross, R. P., and Hill, C. (2008) *PLoS Pathog.* **4,** e1000144
19. Donia, M. S., Ravel, J., and Schmidt, E. W. (2008) *Nat. Chem. Biol.* **4,** 341–343
20. Igarashi, Y., Kan, Y., Fujii, K., Fujita, T., Harada, K., Naoki, H., Tabata, H., Onaka, H., and Furumai, T. (2001) *J. Antibiot.* (*Tokyo*) **54,** 1045–1053
21. Onaka, H., Tabata, H., Igarashi, Y., Sato, Y., and Furumai, T. (2001) *J. Antibiot.* (*Tokyo*) **54,** 1036–1044
22. Schmidt, E. W., Nelson, J. T., Rasko, D. A., Sudek, S., Eisen, J. A., Haygood, M. G., and Ravel, J. (2005) *Proc. Natl. Acad. Sci. U. S. A.* **102,** 7315–7320
23. Williams, A. B., and Jacobs, R. S. (1993) *Cancer Lett.* **71,** 97–102
24. Humar, D., Datta, V., Bast, D. J., Beall, B., De Azavedo, J. C., and Nizet, V. (2002) *Lancet* **359,** 124–129
25. Fuller, J. D., Camus, A. C., Duncan, C. L., Nizet, V., Bast, D. J., Thune, R. L., Low, D. E., and De Azavedo, J. C. (2002) *Infect. Immun.* **70,** 5730–5739
26. Locke, J. B., Colvin, K. M., Varki, N., Vicknair, M. R., Nizet, V., and Buchanan, J. T. (2007) *Dis. Aquat. Organ* **76,** 17–26
27. Bernheimer, A. W. (1949) *J. Exp. Med.* **90,** 373–392
28. Bernheimer, A. W. (1950) *J. Exp. Med.* **92,** 129–132
29. Bernheimer, A. W., and Schwartz, L. L. (1965) *J. Bacteriol.* **89,** 1387–1392
30. Koyama, J. (1963) *J. Biochem.* (*Tokyo*) **54,** 146–151
31. Koyama, J. (1964) *J. Biochem.* (*Tokyo*) **56,** 355–360
32. Koyama, J., and Egami, F. (1963) *J. Biochem.* (*Tokyo*) **53,** 147–154
33. Bernheimer, A. W. (1967) *J. Bacteriol.* **93,** 2024–2025
34. Kelleher, N. L., Hendrickson, C. L., and Walsh, C. T. (1999) *Biochemistry* **38,** 15623–15630
35. Roy, R. S., Allen, O., and Walsh, C. T. (1999) *Chem. Biol.* **6,** 789–799
36. Ginsburg, I., Harris, T. N., and Grossowicz, N. (1963) *J. Exp. Med.* **118,** 905–917
37. Ginsburg, I., Bentwich, Z., and Harris, T. N. (1965) *J. Exp. Med.* **121,** 633–645
38. Li, B., Yu, J. P., Brunzelle, J. S., Moll, G. N., van der Donk, W. A., and Nair, S. K. (2006) *Science* **311,** 1464–1467
39. Okeley, N. M., Paul, M., Stasser, J. P., Blackburn, N., and van der Donk, W. A. (2003) *Biochemistry* **42,** 13613–13624